TechRxiv
Powered by IEEE

# Waveform Design with Constellation Extension for OFDM Dual-Functional Radar-Communications

This paper was downloaded from TechRxiv (https://www.techrxiv.org).

LICENSE

CC BY-NC-SA 4.0

SUBMISSION DATE / POSTED DATE

21-11-2022 / 28-11-2022

CITATION

Memisoglu, Ebubekir; Yılmaz, Talha; Arslan, Hüseyin (2022): Waveform Design with Constellation Extension for OFDM Dual-Functional Radar-Communications. TechRxiv. Preprint.
https://doi.org/10.36227/techrxiv.21592185.v1

DOI

10.36227/techrxiv.21592185.v1

# Waveform Design with Constellation Extension for OFDM Dual-Functional Radar-Communications

Ebubekir Memisoglu, Talha Yılmaz, and Hüseyin Arslan, *Fellow, IEEE*

***Abstract*—Orthogonal frequency division multiplexing (OFDM) is widely used and works efficiently for the communication, but emerging applications requires OFDM to be flexible to meet sensing requirements. The time-frequency waveform design of OFDM for dual-functional radar-communications (DFRC) is critical to achieve the future communication and sensing requirements. Therefore, we propose a novel method to minimize Cramér-Rao bounds (CRBs) of the delay and Doppler estimation to improve radar performance of an OFDM DFRC system. Although some methods are proposed in the literature to improve the CRBs, these methods either require feedforward signaling or subcarrier reservation. However, it is possible to exploit the constellation extension of quadrature amplitude modulation (QAM) to achieve lower CRBs without these requirements. Therefore, the proposed method provides a transparent communication along with the CRB minimization for conventional OFDM systems. For the evaluation of the proposed method, CRB and symbol error rate (SER) are considered in the simulation results. Furthermore, the theoretical SER analysis of the proposed method is derived to understand the effects of CRB minimization on the communication performance.**

***Index Terms*—OFDM, dual-function radar-communications, waveform design, constellation extension, QAM, power optimization, CRB.**

## I. Introduction

FAST development of wireless devices and new applications have drastically increased the wireless data traffic, and current wireless networks cannot comply with the upcoming challenges [1]. Thus, to satisfy the demanding requirements of the new services and applications, wireless communication systems had to extend their capabilities further into the frequency spectrum to access larger amounts of bandwidth [2]–[4]. The spectral expansion of wireless technologies has started to overlap with radar operating bands, causing a great spectrum scarcity [5]–[8]. Furthermore, various applications such as future cellular networks [9], vehicular networks [10], [11], and indoor mapping [12], [13] requires sensing capabilities as well as advanced wireless communication capabilities. Motivated by the reasons above joint radar-communications (JRC) research has gathered great attention. In particular, JRC research consists of two main perspectives; radar-communication coexistence (RCC) and dual-functional radar-communications (DFRC) [5]. RCC aims at developing efficient interference management techniques, so that the radar and communication systems can operate without unduly interfering with each other. On the other hand, DFRC techniques are focused on designing joint systems that can simultaneously perform wireless communication and remote sensing. While RCC approaches require sharing of information between radar and communication systems, or rely on existence of a control center with the coordination capability, DFRC approaches allow for easier cooperation, and decongest the RF environment by using the same signal for both radar and communication functionalities. The authors in [14]–[16] propose RCC systems utilizing orthogonal coexistence, non-orthogonal multiple access (NOMA), and multiple-input multiple-output (MIMO), respectively.

Due to orthogonal frequency division multiplexing (OFDM)'s great performance under frequency selective channels, robust synchronization [17], [18], and native MIMO support OFDM continues to be the cornerstone of current wireless communication standards. Nevertheless, as in conventional OFDM systems, high peak-to-average power ratio (PAPR) is one of the main drawbacks for the OFDM DFRC systems. However, various techniques are already developed to overcome this drawback, such as coding and tone reservation [19]–[21]. Since PAPR is shown to be manageable and OFDM's communication performance is coupled with high accuracy radar operation [22]–[24], OFDM is an excellent candidate as a DFRC waveform. Motivated by the above reasons, there are many proposed DFRC waveform designs on conventional OFDM systems [25]–[35]. Authors in [25] use spectral nulling technique to design DFRC waveform by minimizing peak side-lobes (PSL) in the time domain. Some other waveform designs optimize power allocation across subcarriers by jointly considering achievable capacity and various radar performance metrics [26]–[30]. Specifically [26] and [27] studies waveform design by optimizing mutual information (MI) for radar performance, authors in [28] propose a design regarding Cramér-Rao bound (CRB), and proposed design in [29] optimizes signal-to-noise power ratio (SNR) while [30] features false alarm probability as their optimization radar metric. In recent literature, joint subcarrier selection and power allocation strategies for DFRC waveform design are developed in [31]–[35]. Waveform designs that adopted subcarrier selection and power allocation approaches are classified on which radar metric they have considered. MI based approaches include [31]–[33] while the most recent works [34] and [35] proposed CRB minimized optimal waveforms.

In the subcarrier selection and power allocation approach,

The work of H. Arslan was supported by the Scientific and Technological Research Council of Turkey (TUBITAK) under Grant 120C142.

E. Memisoglu, T. Yılmaz, and H. Arslan are with the Department of Electrical and Electronics Engineering, Istanbul Medipol University, 34810 Istanbul, Turkey. E-mail: ebubekir.memisoglu@std.medipol.edu.tr, {talha.yilmaz, huseyinarslan}@medipol.edu.tr

optimum power allocation for selected radar and communication subcarriers is done through formulated optimization problems based on the adopted scenario. However, proposed joint subcarrier selection and power allocation based methods either exploits certain opportunities like low traffic load in [34] or requires standards support due to novel signalling approaches such as proposed in [35]. Moreover, CRB-based formulations generally yield non-convex problems [31] which leads into computationally expensive solutions.

Motivated by the drawbacks above, this paper proposes a novel OFDM DFRC waveform design inspired by active constellation extension [36]. The proposed approach considers a similar optimization problem for waveform design in [34] and [35], and offers a novel method for the waveform design with constellation extension in DFRC systems. The main contributions of this work are summarized as follows:

- A transparent waveform design to the communication receiver in DFRC systems is proposed, which can be implemented directly in the current wireless standards.
- An unique power allocation method for waveform design is proposed where only the power levels of the data symbols that has been modulated with the outer points of the constellation is enhanced, resulting with improved communication and radar performance.
- A novel method is developed to find the subcarrier indices for the power enhancement in the waveform design.
- Symbol error rate (SER) expressions are derived analytically for the designed waveform to analyze the impact of the proposed algorithm on the communication performance in the OFDM DFRC system.

The rest of the paper is organized as follows. Section II collectively describes the considered DFRC system and signal model. Section III provides the mathematical expressions of delay and Doppler CRBs and explains the proposed waveform design. Section IV derives the theoretical SER expressions for performance analysis of the proposed waveform design. Section V provides simulation results for the evaluation of radar and communication performance. Finally, Section VI concludes this paper. [1]

## II. System Model

A DFRC system for a vehicular wireless communication is considered as described in Fig. 1. The transceiver concurrently transmits OFDM symbols to a communication receiver with single antenna and senses the radar parameters of range and velocity using the reflected signals from radar targets in the environment. Since the transmitter and radar receiver operates on a single hardware, the properties of transmitted signal are perfectly known by radar receiver. Also, a DFRC transceiver with ideal transmitter-receiver isolation is assumed where the self interference due to full duplex radar process can be cancelled significantly by available techniques in the literature [37], [38].

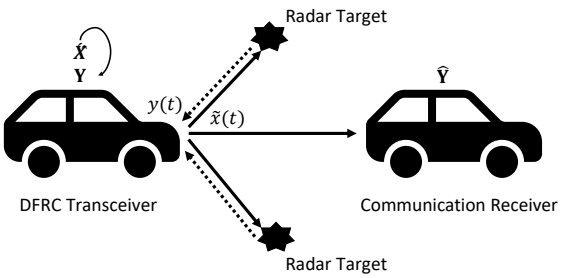



Fig. 1: The considered system model with DFRC transceiver, communication receiver, and radar targets.

### A. Transmit Signal Model

A frame of OFDM waveform is generated to perform communication and radar-sensing concurrently. This frame consists of $M$ OFDM symbols and $N$ subcarriers per each symbol. Here, the symbol duration and subcarrier spacing is denoted by $T$ and $\Delta f = 1/T$, respectively. On the $n$-th subcarrier of $m$-th symbol, the modulated complex data symbols of $D$-quadrature amplitude modulation (QAM) are represented by $X(n,m)$. Then, the $m$-th baseband OFDM signal with a cyclic prefix (CP) addition is given as

$$x_m(t) = \sqrt{\frac{1}{N}} \sum_{n=0}^{N-1} X(n,m) e^{j2\pi n(t-T_{cp})/T} \mathrm{rect}\left(\frac{\mathrm{t}-\mathrm{mT_s}}{\mathrm{T_s}}\right), \tag{1}$$

where $T_{cp}$ and $T_s = T + T_{cp}$ denote the CP duration and the total OFDM symbol duration, respectively. The rectangular function $\mathrm{rect(t)}$ takes the value 1 for $t \in [0, T_s]$ and 0 otherwise. Also, the $T_{cp}$ duration is larger than the maximum excess delay of the communication and radar channel to maintain circular convolution and avoid inter-symbol interference. In the proposed method, the power level of $X(n,m)$ is increased to decrease the delay and Doppler CRBs so that the modified baseband signal is written as

$$\acute{x}_m(t) = \sqrt{\frac{1}{N}} \sum_{n=0}^{N-1} \acute{X}(n,m) e^{j2\pi n(t-T_{cp})/T} \mathrm{rect}\left(\frac{\mathrm{t}-\mathrm{mT_s}}{\mathrm{T_s}}\right), \tag{2}$$

where the transmit power on the $n$-th subcarrier of $m$-th symbol is represented as $P(n,m) = |\acute{X}(n,m)|^2$. Here, the conventional OFDM system has the transmit power level of $P(n,m) = |X(n,m)|^2$. Then, the baseband signal is converted to the passband signal and transmitted via an antenna as

$$\tilde{x}(t) = \Re\left\{\sum_{m=0}^{M-1} \acute{x}_m(t) e^{j2\pi f_c t}\right\}, \tag{3}$$

[1] *Notation:* Bold, lowercase and capital letters denote the signal vectors and matrices, respectively. $\Re\{.\}$ is the real part of a complex signal. $(.)^T$ and $(.)^H$ denote transposition and Hermitian transposition, respectively. $\odot$ and $\otimes$ denote the Hadamard and tensor product, respectively. $\mathbf{1}_M$ is an one vector with the size $M$. $\mathcal{CN}(0,\sigma^2)$ denotes the circularly symmetric complex Gaussian distribution with 0 mean and variance $\sigma^2$. $\|.\|_\infty$ denotes the infinity norm of a vector. The floor function is denoted by $\lfloor . \rfloor$. The function vec(.) converts a matrix into vector form. The function $sort(.)$ sorts the elements of a vector in ascending order and returns the sorted vector. The function $mod(a,m)$ returns the remainder after division of $a$ by $m$, where $a$ is the dividend and $m$ is the divisor. The complementary error function is denoted by $Q(x) = \int_x^\infty \frac{2}{\sqrt{\pi}} e^{-x^2} dx$.

where $f_c$ is the carrier frequency of the transmitted signal.

### B. Radar Receiver

Suppose there are $K$ radar targets in the environment. The reflected signal from the $k$-th target is received with a delay $\tau_k$ and normalized Doppler shift $\nu_k \triangleq 2v_k/c$ where $v_k$ and $c$ are the radial velocity and the speed of propagation, respectively. The reflected signal has an attenuation factor $h_k$ including path loss, reflection and processing gains. Then, after down-conversion operation, the downconverted signal at the radar receiver can be expressed as [39]

$$\begin{aligned} y(t) &= \sum_{k=0}^{K-1}\sum_{m=0}^{M-1} h_k \acute{x}_m(t-\tau_k)e^{j2\pi f_c \nu_k t} + w(t), \\ &\approx \sum_{k=0}^{K-1}\sum_{m=0}^{M-1} h_k \acute{x}_m(t-\tau_k)e^{j2\pi f_c \nu_k m T_s} + w(t), \end{aligned} \tag{4}$$

where $w(t)$ is the additive noise and the approximation in (4) is done by assuming $f_c \nu_k T_s \ll 1$ so that the phase rotation within one OFDM symbol is approximately constant. After the CP removal, the Fourier transform is applied to the $m$-th OFDM symbol and then the received signal in the frequency domain is obtained as [39]

$$\begin{aligned} Y(n,m) = \acute{X}(n,m) \sum_{k=0}^{K-1} \alpha_k e^{-j2\pi n \Delta f \tau_k} e^{j2\pi f_c \nu_k m T_s} \\ + Z(n,m), \end{aligned} \tag{5}$$

where $\alpha_k = h_k T$ and $Z(n,m)$ is the additive white Gaussian noise (AWGN) sample with $\mathcal{CN}(0,\, \sigma_r^2)$. Denoting the frequency and time steering vectors as

$$\boldsymbol{\theta}(\tau) \triangleq [1, e^{-j2\pi\Delta f\tau}, \ldots, e^{-j2\pi(N-1)\Delta f\tau}]^T, \tag{6}$$

$$\boldsymbol{\phi}(\nu) \triangleq [1, e^{-j2\pi f_c T_s \nu}, \ldots, e^{-j2\pi f_c (M-1) T_s \nu}]^T. \tag{7}$$

Accordingly, plugging (6) and (7) into (5), the received signal in matrix form can be written as

$$\mathbf{Y} = \acute{\mathbf{X}} \odot \sum_{k=0}^{K-1} \alpha_k \boldsymbol{\theta}(\tau_k)\boldsymbol{\phi}^H(\nu_k) + \mathbf{Z}, \tag{8}$$

where $\mathbf{Y} \in \mathbb{C}^{N\times M}$, $\acute{\mathbf{X}} \in \mathbb{C}^{N\times M}$ and $\mathbf{Z} \in \mathbb{C}^{N\times M}$ are the matrices of $Y(n,m)$, $\acute{X}(n,m)$ and $Z(n,m)$, respectively.

### C. Communication Receiver

After the down-conversion of the received signal to baseband, the CP removal and fast Fourier transform (FFT) operations are performed for each OFDM symbol at the communication receiver. Then, the received signal in the frequency domain similar to (8) can be written as

$$\widehat{\mathbf{Y}} = \acute{\mathbf{X}} \odot \widehat{\mathbf{H}} + \widehat{\mathbf{Z}}, \tag{9}$$

where $\widehat{\mathbf{H}} \in \mathbb{C}^{N\times M}$ represents Rayleigh channel frequency response factors of the communication channel with $\mathcal{CN}(0,\, 1)$ and $\widehat{\mathbf{Z}} \in \mathbb{C}^{N\times M}$ is the AWGN matrix with $\mathcal{CN}(0,\, \sigma_c^2)$. At communication receiver, a perfect channel state information is assumed for channel equalization. The equalized data symbols are decoded to obtain the transmitted data symbols. Although a perfect channel state information is considered at the communication receiver in the system model, an imperfect channel state information will have a same degradation for conventional OFDM and proposed method because the proposed method only modify the data symbols, not the pilot symbols. As a result, channel estimation performance will be identical for conventional OFDM and proposed method.

## III. Waveform Design

In this section, the calculation of the delay and Doppler CRBs are provided and the proposed waveform design is explained in detail.

### A. CRBs of Delay and Doppler Estimation

Proposed waveform design considers delay and Doppler CRBs to improve radar performance. The waveform design to increase the radar performance by minimizing the CRBs requires a proper power allocation. The power level of data symbols in the frame are represented by the matrix $\mathbf{P}$, and the vector form of $\mathbf{P}$ is denoted as $\mathbf{q} \triangleq \mathrm{vec}\,(\mathbf{P})$. Then, the CRBs of unbiased estimates $\widehat{\tau}$ and $\widehat{\nu}$ for delay and Doppler estimation in single target case can be calculated as [35]

$$\mathrm{var}\,(\widehat{\tau}) \geq \mathrm{C}_\tau = \frac{1}{2\gamma_r} \frac{(\mathbf{1}^T\mathbf{q})(\mathbf{q}^T\boldsymbol{\Upsilon}_\nu\mathbf{q})}{(\mathbf{q}^T\boldsymbol{\Upsilon}_\tau\mathbf{q})(\mathbf{q}^T\boldsymbol{\Upsilon}_\nu\mathbf{q}) - (\mathbf{q}^T\boldsymbol{\Upsilon}_{\tau\nu}\mathbf{q})^2}, \tag{10}$$

$$\mathrm{var}\,(\widehat{\nu}) \geq \mathrm{C}_\nu = \frac{1}{2\gamma_r} \frac{(\mathbf{1}^T\mathbf{q})(\mathbf{q}^T\boldsymbol{\Upsilon}_\tau\mathbf{q})}{(\mathbf{q}^T\boldsymbol{\Upsilon}_\tau\mathbf{q})(\mathbf{q}^T\boldsymbol{\Upsilon}_\nu\mathbf{q}) - (\mathbf{q}^T\boldsymbol{\Upsilon}_{\tau\nu}\mathbf{q})^2}, \tag{11}$$

where

$$\begin{aligned} \mathbf{u}_\tau &\triangleq 2\pi\Delta f(\mathbf{1}_M \otimes \xi_N), \\ \mathbf{u}_\nu &\triangleq 2\pi f_c T_s(\xi_M \otimes \mathbf{1}_N), \\ \boldsymbol{\Upsilon}_\tau &\triangleq (\mathbf{u}_\tau \odot \mathbf{u}_\tau)\,\mathbf{1}_{NM}^T - \mathbf{u}_\tau\mathbf{u}_\tau^T, \\ \boldsymbol{\Upsilon}_\nu &\triangleq (\mathbf{u}_\nu \odot \mathbf{u}_\nu)\,\mathbf{1}_{NM}^T - \mathbf{u}_\nu\mathbf{u}_\nu^T, \\ \boldsymbol{\Upsilon}_{\tau\nu} &\triangleq (\mathbf{u}_\tau \odot \mathbf{u}_\nu)\,\mathbf{1}_{NM}^T - \mathbf{u}_\tau\mathbf{u}_\nu^T. \end{aligned}$$

Here, $\gamma_r$ is the SNR at the radar receiver and $\xi_N = [0, 1, \ldots, N-1]$. As seen from (10) and (11), the CRBs depend on $\mathbf{q}$, $\gamma_r$, $\Delta f$, $f_c$, and $T_s$. Since the parameters of $\gamma_r$, $\Delta f$, $f_c$, and $T_s$ are system parameters for a target delay and Doppler estimation, only $\mathbf{q}$ is changed for the CRBs minimization in the waveform design.

### B. Proposed Waveform Design

The minimization of the joint delay and Doppler CRBs involves optimization of the OFDM subcarrier powers. In conventional OFDM systems, the $\mathbf{P}$ matrix is formed by the power of the modulated data symbols based on the $D$-QAM, and they have a total power of $P_c$. On the other hand, since the power of data symbols are increased to improve the radar performance by minimizing the CRBs, the data symbols in the frame will have a total power of $P_t$ where $P_t > P_c$. In the proposed waveform design, only OFDM

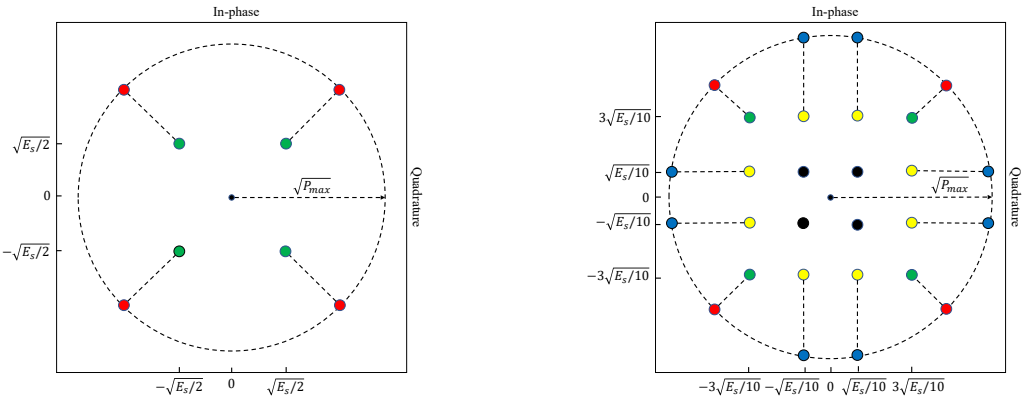



Fig. 2: The scatter plots of the proposed waveform design for QPSK and 16-QAM constellation. The black, yellow and green circles belong to conventional constellation, and blue and red circles are due to the proposed method.

data symbols are used for the power optimization. Therefore, separate subcarriers as in [34] are not assigned for the radar performance improvement. Also, a power threshold $P_{max}$ for data symbols is considered in the CRB minimization for the following reasons: Firstly, the transmit signal requires to be a spectrum mask compliant. Accordingly, if there is a large power difference between subcarriers, the average signal power needs to be decreased so that the subcarriers with highest power level are compliant with spectrum mask. However, this will not be a power efficient. Secondly, if there is an inter-carrier interference in the system, the interference of high power subcarriers affects other subcarriers significantly for the communication performance. Lastly, if the ratio of the maximum power to the average power increases, the side-lobe level of ambiguity function also increases [40].

Owing to the fact that there are the constraints of $P_t$ and $P_{max}$ in the system for optimum CRB minimization, the subcarrier indices to obtain the optimum CRBs need to be found for the power allocation. These subcarrier indices are represented with the set $R_m$ for the $m$-th OFDM symbol and the subcarriers in $R_m$ have power allocation of $P_{max}$. Therefore, the power allocation problem for the optimum CRB minimization can be formulated as

$$\min_{\mathbf{q}} \quad \lambda C_\tau + (1-\lambda) C_\nu \tag{12a}$$

$$\text{s.t.} \quad \mathbf{1}_{NM}^T \mathbf{q} = P_t, \quad \mathbf{q} \succeq 0, \tag{12b}$$

$$\|\mathbf{q}\|_\infty = P_{max}, \tag{12c}$$

$$P(n,m) = P_{max}, \ n \in R_m, \ \forall m, \tag{12d}$$

where $\lambda$ denotes the determined weighting factor for delay Doppler estimation accuracy. For instance, if $\lambda = 1$, the optimization only minimizes the CRB for the delay estimation. Note that there is a relationship between $\mathbf{q}$ and $\mathbf{P}$ as $\mathbf{q} \triangleq \text{vec}(\mathbf{P})$. As deduced from (12a), the $R_m$ set requires to be found and then the power allocation to the subcarrier indices in $R_m$ is performed to obtain $\mathbf{q}$.

The power allocation to data symbols of $D$-QAM on the selected subcarriers for the proposed method is illustrated for the quadrature phase shift keying (QPSK) and 16-QAM constellation in Fig. 2. The symbol alphabet of $D$-QAM is defined as $\mathcal{S} = \{\pm(2d+1) \pm (2d+1)j\}$ with $d = \{0, 1, \ldots, \sqrt{D}/2-1\}$. For the power allocation in the proposed method, $\mathcal{S}$ is divided into three subsets as $\mathcal{S}_1$, $\mathcal{S}_2$ and $\mathcal{S}_3$. The subsets $\mathcal{S}_1$, $\mathcal{S}_2$ and $\mathcal{S}_3$ have the data points of the $D$-QAM constellation in the inside (black colored circles), in the corner (green colored circles), and neither in the inside nor in the corner (yellow colored circles), respectively. As seen from the figure, the power levels of data points in $\mathcal{S}_2$ and $\mathcal{S}_3$ are increased in the proposed method. Therefore, the sets of empowered data symbols of $\mathcal{S}_2$ and $\mathcal{S}_3$ are denoted by $\mathcal{C}_1$ (red colored circles) and $\mathcal{C}_2$ (blue colored circles), respectively. The data symbols of $D$-QAM constellation have the average power of $E_s$ and the normalization factor is calculated as $\sqrt{(2(D-1)/3)}$.

To design the $\mathbf{q}$ vector for the optimum CRB minimization, firstly, the total number of subcarriers for the power allocation is required to be determined. The number depends on the parameters of $P_c$, $P_t$, $P_{max}$ and $D$-QAM. In the proposed method, the power levels of only data symbols in $\mathcal{S}_2$ and $\mathcal{S}_3$ are increased. The power levels of the $d_2$-th and $d_3$-th data symbol in $\mathcal{S}_2$ and $\mathcal{S}_3$ are represented by $P_{d_2}$ and $P_{d_3}$ where $d_2 = \{0, 1, \ldots, D_2 - 1\}$ and $d_3 = \{0, 1, \ldots, D_3 - 1\}$, respectively. Therefore, the total number of subcarriers with a $P_{max}$ power level can be calculated as

$$N_R = \left\lfloor \frac{(P_t - P_c)(D_2 + D_3)}{\sum_{d_2=0}^{D_2-1}(P_{max} - P_{d_2}) + \sum_{d_3=0}^{D_3-1}(P_{max} - P_{d_3})} \right\rfloor. \tag{13}$$

The probability of a data symbol in $\mathcal{S}_2 \cup \mathcal{S}_3$ is calculated as $\frac{1}{(D_2+D_3)}$. For instance, QPSK constellation has the parameters of $D_2 = 4$ and $D_3 = 0$, and the probability of $\frac{1}{4}$, on the other hand, the 16-QAM constellation has the parameters of $D_2 = 4$ and $D_3 = 8$, and the probability of $\frac{1}{12}$ as seen from Fig. 2. In the case of constant $P_t$, $P_c$ and $D$, if $P_{max}$ increases, $N_R$ decreases.

After calculating the $N_R$, the $N_R$ subcarrier indices among $MN$ subcarrier indices are required to be selected for an optimum CRB optimization. Then, the proposed method allocates a power level of $P_{max}$ to the selected subcarriers. Note that

**Algorithm 1** The matrix generation of weight factors.

Define $f_c$, $\Delta f$, $T_{sym}$, $\gamma_r$, $N$, $M$, $P_{max}$ and $\lambda$
Set $n = 0$
**while** $n \leq N-1$ **do**
  Set $m = 0$
  **while** $m \leq M-1$ **do**
    $\bar{\mathbf{P}} = \mathbf{1}_{N\times M}$
    $\bar{P}(n,m) = P_{max}$
    $\bar{\mathbf{q}} \triangleq \text{vec}\left(\bar{\mathbf{P}}\right)$
    $G(n,m) = \lambda C_\tau + (1-\lambda)C_\nu$
    $m \leftarrow m+1$
  **end while**
  $n \leftarrow n+1$
**end while**

**Algorithm 2** Proposed waveform design.

Define $P_t$, $P_c$, $N$, $M$, $P_{max}$ and $D$
Set $i = 0$ and $\acute{\mathbf{X}} = \mathbf{X}$
Calculate $N_R$ in (13)
Find the $\mathbf{G}$ matrix by Algorithm 1
**while** $i \leq N_R - 1$ **do**
  $\mathbf{g} \triangleq \text{vec}\left(\mathbf{G}\right)$
  $[\acute{\mathbf{g}}, \mathbf{I}] = sort(\mathbf{g})$
  $n = mod(I(i), N)$
  $m = \lfloor (I(i))/M \rfloor$
  **if** $X(n,m) \in \mathcal{S}_2$ **then**
    $\acute{X}(n,m) = \sqrt{P_{max}}\frac{X(n,m)}{|X(n,m)|}$
  **elseif** $X(n,m) \in \mathcal{S}_3$ **then**
    $\acute{X}(n,m) = X(n,m) + A_{d_3}$
  **else**
    $\acute{X}(n,m) = X(n,m)$
  **end if**
  $i \leftarrow i+1$
**end while**

$P_{max}$ is always larger than the power of the data symbols on the selected subcarrier. To find the optimum $\mathbf{q}$ in Eq. (12a), the number of different combinations for brute-force search is calculated as $\frac{(MN)!}{N_R!(MN-N_R)!}$. Therefore, the brute-force search is not feasible in a practical system. For instance, the approximate number of $4.48\times10^{306}$ searches are required to find the optimum $\mathbf{q}$ vector with brute-force search for the parameters of $N = 64$, $M = 16$, and $N_R = 512$. Also, the problem in (12a) is not a convex problem. Therefore, a sub-optimal search method is developed to design $\mathbf{q}$. As inferred from Eqs. (10) and (11), all subcarriers are independent of each other and the power enhancement of each subcarrier contributes to the CRB minimization positively. It means that the power enhancement of any subcarrier minimizes the CRBs of delay and Doppler estimation. However, the power enhancement of each subcarrier contributes differently on the CRB minimization. This feature is also mentioned in [34] and [35]. For instance, the edge-most subcarriers are better for the delay CRB minimization, on the other hand, the edge-most OFDM symbols are better for the Doppler CRB minimization [34]. Therefore, the weighting factors for the CRB minimization are calculated to select the $N_R$ subcarrier indices as a suboptimal solution.

The matrix $\mathbf{G} \in \mathbb{R}^{N\times M}$ of the weight factors is formed as described in Algorithm 1. Firstly, the system parameters of $f_c$, $\Delta f$, $T_s$, $\gamma_r$, $N$, $M$, $P_{max}$ and $\lambda$ are determined. If the system parameters are constant for a different frame generation, same $\mathbf{G}$ matrix can be used to select the subcarrier indices for CRB minimization. For a fair evaluation, a unit power level is assigned to all subcarriers in the beginning as $\bar{\mathbf{P}} = \mathbf{1}_{N\times M}$. Then, the power level of the $n$-th subcarrier of the $m$-th OFDM symbol is increased to $P_{max}$ as $\bar{P}(n,m) = P_{max}$. Next, the $\bar{\mathbf{P}}$ matrix is vectorized to $\bar{\mathbf{q}} \triangleq \text{vec}\left(\bar{\mathbf{P}}\right)$. Afterwards, according to the minimization problem in (12a), the weight factor for the $n$-th subcarrier of the $m$-th OFDM symbol is found as $G_{n,m} = \lambda C_\tau + (1-\lambda)C_\nu$. Note that only one element with $P_{max}$ is available in $\bar{\mathbf{q}}$, and other elements have unit power level for each iteration. After finding the weight factors for each subcarrier indices in the frame, the matrix $\mathbf{G}$ is formed. Since the matrix $\mathbf{G}$ indicates the performance of CRB minimization for the subcarrier indices, the indices with lower values in $\mathbf{G}$ are more efficient for the minimization problem in (12a).

The CRB improvement for better radar performance is achieved by increasing the power level of subcarriers in $\mathbf{X}$ for the proposed method. The proposed method exploits the modulation constellation to increase the power level of data symbols, and provides a transparent operation to the communication receiver as in [36]. Therefore, same processes at the receiver with conventional OFDM systems are required for the proposed method. To achieve this, the proposed method only increases the power levels of data symbols in $\mathcal{S}_2 \cup \mathcal{S}_3$ as shown in Fig. 2. In the figure, the constellations of QPSK and 16-QAM are described. For the QPSK modulation, all data symbols are on the outer of the constellation so that all subcarriers in $\mathbf{X}$ are suitable for the power enhancement. Hence, if the data symbols on the constellation diagram have same power level and different phases as in phase shift keying modulation, the proposed method can use all data symbols for the power enhancement. On the other hand, if the data symbols on the constellation diagram have different power levels and phases as in 16-QAM, only the outer data symbols in $\mathcal{S}_2 \cup \mathcal{S}_3$ can be used to minimize the CRB.

The proposed waveform design is performed as described in Algorithm 2. In the algorithm, firstly, the system parameters of $P_t$, $P_c$, $N$, $M$, $P_{max}$ and $D$ are determined. After calculating $N_R$ in (13) and finding the $\mathbf{G}$ matrix in Algorithm 1, the power enhancement of $N_R$ subcarriers starts. To find the $\mathbf{q}$ in the proposed method, the subcarrier indices according to $\mathbf{G}$ should be sorted. For the sorting, the vector form of $\mathbf{G}$ as $\mathbf{g} \triangleq \text{vec}\left(\mathbf{G}\right)$ is used. The corresponding indices of $\mathbf{g}$ as $\bar{\mathbf{g}} \in \mathbb{R}^{NM\times1}$ and $\mathbf{I} \in \mathbb{N}^{NM\times1}$, respectively. The indices of the $i$-th subcarrier for the power enhancement in the terms of $n$ and $m$ are calculated as $n = mod(I(i), N)$ and $m = \lfloor I(i)/M \rfloor$, where $i = \{0, 1, \ldots, NM-1\}$. Afterwards, check the data symbol on $X(n,m)$, if it is in $\mathcal{S}_2$, then change its power level to $P_{max}$ as $\acute{X}(n,m) = \sqrt{P_{max}}\frac{X(n,m)}{|X(n,m)|}$. If it is in $\mathcal{S}_3$, add a complex value $A_{d_3}$ to $X(n,m)$ for the $d_3$-th data symbol in $\mathcal{S}_3$ so that $\acute{X}(n,m) = X(n,m) + A_{d_3}$ have the power level of $P_{max}$. If it is in $\mathcal{S}_1$, do not change the power level as $\acute{X}(n,m) = X(n,m)$. After the power levels of data symbols on the $N_R$ subcarriers are increased, the matrix $\acute{\mathbf{X}}$ is obtained. Note that the modifications on $\mathbf{X}$ to obtain $\acute{\mathbf{X}}$ optimize $\mathbf{q}$ in

Eq. (12a) and are transparent to the communication receiver. Therefore, if the system requires to enhance radar performance by minimizing the CRBs of delay and Doppler estimations, the proposed method can meet this requirement without a channel state information at the DFRC transceiver and a feedforward signaling to the communication receiver.

## IV. Performance Analysis

In this section, the theoretical SER analysis is investigated. Firstly, the averaged SER of conventional OFDM is provided, then the average SER of the proposed method is obtained.

The received signal on the $n$-th subcarrier of $m$-th conventional OFDM symbol at the communication receiver is given as

$$\widehat{Y}(n,m) = X(n,m)\widehat{H}(n,m) + \widehat{Z}(n,m), \tag{14}$$

where the probability distribution function of the Gaussian random variable $z = \Re\{\widehat{Z}(n,m)\}$ with the 0 mean and variance $\sigma_c^2/2$ is

$$p(z) = \frac{1}{\sqrt{\pi\sigma_c^2}} e^{-\frac{z^2}{\sigma_c^2}}. \tag{15}$$

Then, the instantaneous SNR can be written as

$$\gamma_c(n,m) = \frac{|X(n,m)|^2 |\widehat{H}(n,m)|^2}{\sigma_c^2}. \tag{16}$$

Afterwards, the average SNR per data symbol is found by taking the expected value of (16) as $\bar{\gamma}_c = \frac{E_s}{\sigma_c^2}$. After the $\bar{\gamma}_c$ is obtained, the closed-form expression of average SER for $D$-QAM over Rayleigh fading channels is given as [41]

$$P_s(E) = 2\left(\frac{\sqrt{D}-1}{\sqrt{D}}\right)(1-\beta) - \left(\frac{\sqrt{D}-1}{\sqrt{D}}\right)^2 \left[1 - \beta\left(\frac{4}{\pi} tan^{-1}\left(\frac{1}{\beta}\right)\right)\right], \tag{17}$$

where $\beta = \sqrt{\frac{1.5\bar{\gamma}_c}{D-1+1.5\bar{\gamma}_c}}$.

In the constellation of the proposed method, the data symbols belong to the sets of $\mathcal{S}_1$, $\mathcal{S}_2$, $\mathcal{S}_3$, $\mathcal{C}_1$ and $\mathcal{C}_2$. As seen from Fig. 3, the data symbols in these sets have different the minimum distances to the decision boundaries and the number of decision boundaries. Therefore, the minimum distances to decision boundaries for the data symbols in $\mathcal{S}_1$, $\mathcal{S}_2$, $\mathcal{S}_3$, $\mathcal{C}_1$ and $\mathcal{C}_2$ are $(l_1, l_1, l_1, l_1)$, $(l_1, l_1)$, $(l_1, l_1, l_1)$, $(l_2, l_2)$, and $(l_1, l_1, |A_{d_3}| + l_1)$ as shown in the figure. The distances of $l_1$ and $l_2$ are calculated as $l_1 = \sqrt{3E_s/(2(D-1))}$ and $l_2 = \sqrt{P_{max}/2} - (\sqrt{D}-2)l_1$. Although each data symbol in $\mathcal{S}_1$, $\mathcal{S}_2$, $\mathcal{S}_3$, and $\mathcal{C}_1$ have same minimum distances to decision boundaries, the data symbols in $\mathcal{C}_2$ may have different minimum distances. However, each data symbol in $\mathcal{C}_2$ have same minimum distances for 16-QAM, and $|A_{d_3}|$ is calculated as $|A_{d_3}| = \sqrt{(P_{max} - l_1^2)} - 3l_1$ for all $d_3$ indices.

To calculate the average SER of the proposed method, firstly, the individual SER of each data symbol on the constellation of $D$-QAM is calculated, and then the average SER is found from the individual SERs. These data symbols belong to the sets of $\mathcal{S}_1$, $\mathcal{S}_2$, $\mathcal{S}_3$, $\mathcal{C}_1$, and $\mathcal{C}_2$. The data symbols on each set except in $\mathcal{C}_2$ have same SER performance. The SERs of $D$-QAM data symbols according to their sets for a channel factor $h = \widehat{H}(n,m)$ are given as [42] [43]

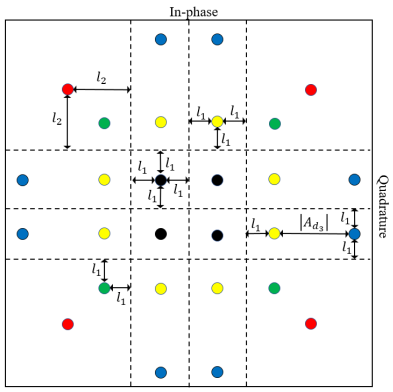



Fig. 3: The minimum distances to the decision boundaries (dashed lines) in the constellation of the proposed method for $D$-QAM.

$$\dot{P}_s(E|\mathcal{S}_1) = 1 - \left(1 - \frac{1}{2}Q\left(\sqrt{\frac{l_1^2|h|^2}{\sigma_c^2}}\right) - \frac{1}{2}Q\left(\sqrt{\frac{l_1^2|h|^2}{\sigma_c^2}}\right)\right) \times \left(1 - \frac{1}{2}Q\left(\sqrt{\frac{l_1^2|h|^2}{\sigma_c^2}}\right) - \frac{1}{2}Q\left(\sqrt{\frac{l_1^2|h|^2}{\sigma_c^2}}\right)\right), \tag{18}$$

$$\dot{P}_s(E|\mathcal{S}_2) = 1 - \left(1 - \frac{1}{2}Q\left(\sqrt{\frac{l_1^2|h|^2}{\sigma_c^2}}\right)\right) \times \left(1 - \frac{1}{2}Q\left(\sqrt{\frac{l_1^2|h|^2}{\sigma_c^2}}\right)\right), \tag{19}$$

$$\dot{P}_s(E|\mathcal{S}_3) = 1 - \left(1 - \frac{1}{2}Q\left(\sqrt{\frac{l_1^2|h|^2}{\sigma_c^2}}\right) - \frac{1}{2}Q\left(\sqrt{\frac{l_1^2|h|^2}{\sigma_c^2}}\right)\right) \times \left(1 - \frac{1}{2}Q\left(\sqrt{\frac{l_1^2|h|^2}{\sigma_c^2}}\right)\right), \tag{20}$$

$$\dot{P}_s(E|\mathcal{C}_1) = 1 - \left(1 - \frac{1}{2}Q\left(\sqrt{\frac{l_2^2|h|^2}{\sigma_c^2}}\right)\right) \times \left(1 - \frac{1}{2}Q\left(\sqrt{\frac{l_2^2|h|^2}{\sigma_c^2}}\right)\right), \tag{21}$$

$$\dot{P}_s(E|\mathcal{C}_2) = 1 - \left(1 - \frac{1}{2}Q\left(\sqrt{\frac{l_1^2|h|^2}{\sigma_c^2}}\right) - \frac{1}{2}Q\left(\sqrt{\frac{l_1^2|h|^2}{\sigma_c^2}}\right)\right) \times \left(1 - \frac{1}{2D_3}\sum_{d_3=0}^{D_3-1} Q\left(\sqrt{\frac{(|A_{d_3}| + l_1)^2|h|^2}{\sigma_c^2}}\right)\right). \tag{22}$$

For conventional $D$-QAM constellation, the data symbols have an equal minimum distance to decision boundaries; however, the distances to the boundaries are different in the proposed method. Thus, the distances of $l_1$ and $l_2$ are calculated as

TABLE I: The parameter values for the OFDM signal.

| **Parameters** | **Values** |
|---|---|
| Carrier frequency ($f_c$) | 2 $GHz$ |
| Number of subcarriers ($N$) | 64 |
| Subcarrier spacing ($\Delta f$) | 23.4 $kHz$ |
| Total symbol duration ($T_s$) | 64 $\mu s$ |
| Number of symbols ($M$) | 16 |
| Number of frames | $10^5$ |
| Average signal power ($E_s$) | 1 |
| Total signal power ($P_c$) | NM |
| Total transmit signal power ($P_t$) | 2NM |

$l_1 = \sqrt{3E_s/(2(D-1))}$ and $l_2 = \sqrt{P_{max}/2} - (\sqrt{D}-2)l_1$. Although $|A_{d_3}|$ may have different values, it has a constant value as $|A_{d_3}| = \sqrt{(P_{max} - l_1^2)} - 3l_1$ for 16-QAM.

Since the Rayleigh fading channel model is considered, the random variable $\varphi = |h|^2$ will has a probability distribution function of chi-square with two degrees of freedom as [43]

$$p(\varphi) = e^{-\varphi}, \quad \varphi \geq 0. \tag{23}$$

Then, the average SER of the data symbols on $\mathcal{S}_1$, $\mathcal{S}_2$, $\mathcal{S}_3$, $\mathcal{C}_1$, and $\mathcal{C}_2$ for a Rayleigh channel are calculated respectively as

$$\widehat{P}_s(E|\mathcal{S}_1) = \int_0^\infty \dot{P}_s(E|\mathcal{S}_1)p(\varphi)d\varphi, \tag{24}$$

$$\widehat{P}_s(E|\mathcal{S}_2) = \int_0^\infty \dot{P}_s(E|\mathcal{S}_2)p(\varphi)d\varphi, \tag{25}$$

$$\widehat{P}_s(E|\mathcal{S}_3) = \int_0^\infty \dot{P}_s(E|\mathcal{S}_3)p(\varphi)d\varphi, \tag{26}$$

$$\widehat{P}_s(E|\mathcal{C}_1) = \int_0^\infty \dot{P}_s(E|\mathcal{C}_1)p(\varphi)d\varphi, \tag{27}$$

$$\widehat{P}_s(E|\mathcal{C}_2) = \int_0^\infty \dot{P}_s(E|\mathcal{C}_2)p(\varphi)d\varphi. \tag{28}$$

To find the overall probability, the average probability of each set in the frame requires. Therefore, the occurrence probabilities of the sets in the frame are calculated as

$$P(\mathcal{S}_1) = \frac{\left(\sqrt{D}-2\right)\left(\sqrt{D}-2\right)}{D}, \tag{29}$$

$$P(\mathcal{S}_2) = \left(1 - P(\mathcal{S}_1) - \frac{N_R}{NM}\right)\left(\frac{1}{1+\sqrt{D}-2}\right), \tag{30}$$

$$P(\mathcal{S}_3) = \left(1 - P(\mathcal{S}_1) - \frac{N_R}{NM}\right)\left(\frac{\sqrt{D}-2}{1+\sqrt{D}-2}\right), \tag{31}$$

$$P(\mathcal{C}_1) = \left(\frac{N_R}{NM}\right)\left(\frac{1}{1+\sqrt{D}-2}\right), \tag{32}$$

$$P(\mathcal{C}_2) = \left(\frac{N_R}{NM}\right)\left(\frac{\sqrt{D}-2}{1+\sqrt{D}-2}\right). \tag{33}$$

Then, the overall average SER is calculated as

$$\begin{aligned}\widehat{P}_s(E) =& P(\mathcal{S}_1)\widehat{P}_s(E|\mathcal{S}_1) + P(\mathcal{S}_2)\widehat{P}_s(E|\mathcal{S}_2) \\ &+ P(\mathcal{S}_3)\widehat{P}_s(E|\mathcal{S}_3) + P(\mathcal{C}_1)\widehat{P}_s(E|\mathcal{C}_1) \\ &+ P(\mathcal{C}_2)\widehat{P}_s(E|\mathcal{C}_2).\end{aligned} \tag{34}$$

## V. Simulation Results

In this section, the simulation results of the proposed waveform design are provided. The parameter values for the simulations are given in Table I. To observe the effects of different modulation orders in the proposed waveform design, QPSK ($D = 4$) and 16-QAM ($D = 16$) are used for the data symbols. The parameters $E_s$, $P_c$, and $P_t$ are assigned based on the values of the QAM symbols in the frame. According to $P_c$ and $P_t$, the different $P_{max}$ values of 2, 3, and 5 are used for the CRB optimization. The radar SNR value is calculated as $\gamma_r = P_t/\sigma_r^2$. For the communication channel, a frequency selective channel with 4 taps is generated.

The performances of CRB optimization of delay and Doppler estimates with $\lambda = 1$ and $\lambda = 0$ are obtained in Fig. 4. Note that the waveform design optimization with $\lambda = 1$ considers the only delay CRB, and if $\lambda = 0$, then only Doppler CRB is considered for the optimization. The $P_{max} = 2$ value is used only for QPSK modulation, and all subcarriers have the $P_{max}$ power level in that case. In the 16-QAM, $P_{max} = 2$ is not a feasible power level because the number of suitable subcarriers for the power enhancement in the proposed method is not sufficient to reach to $P_t$. The reason of using $P_{max} = 2$ is to show the effects of uniform power enhancement in the proposed method. As seen from the figure, if the $P_{max}$ value increases, the CRB metric decreases for both delay and Doppler estimates. Therefore, a larger $P_{max}$ value is better for the CRB minimization, but it should be limited in practical system due the reasons explained in Section III. The performance gains for delay and Doppler CRBs have similar characteristics. For the QPSK modulation, all OFDM data symbols have the same power level, and all of them are suitable for the power enhancement. On the other hand, for the 16-QAM modulation, the data symbols have different power levels although they have the same average power with QPSK. Therefore, the only data symbols on $\mathcal{S}_2$ and $\mathcal{S}_3$ are suitable for the power enhancement. Since some subcarriers indices with unsuitable data symbols are skipped for the power enhancement, the CRB minimization performance with 16-QAM is worse than the QPSK modulation. However, the gain difference decreases for larger $P_{max}$ values.

The effects of $\lambda$ on the CRBs of the proposed method with different modulation orders and $P_{max}$ values are investigated in Fig. 5. If $0 < \lambda < 1$, the joint CRB optimization for delay and Doppler estimation is performed. If $\lambda = 1$, the best delay CRB performance is obtained, on the other hand, if $\lambda = 0$, the best Doppler CRB performance is obtained. The changing $\lambda$ between 0 and 1 such as $\lambda = 1/2$ compromises between delay and Doppler CRB performances. Therefore, the decrease of $\lambda$ increases the delay CRB while the Doppler CRB decreases. The change of CRB performance for a different $\lambda$ value is not same for delay and Doppler estimates, and it depends on the system parameters such as $f_c$, $N$, $M$, and $\Delta f$. As seen from the figure, the change in $\lambda$ affects the CRBs performance more if $P_{max}$ is larger. Moreover, the change in $\lambda$ affects the CRBs performance more if $D$ is smaller.

The average SER performance of the proposed method compared to conventional OFDM are shown in Fig. 6. For symbol detection at the communication receiver, the same processes with conventional OFDM are deployed for the proposed method. As seen from the figure, the power enhancement of the subcarriers for CRB optimization also enhances

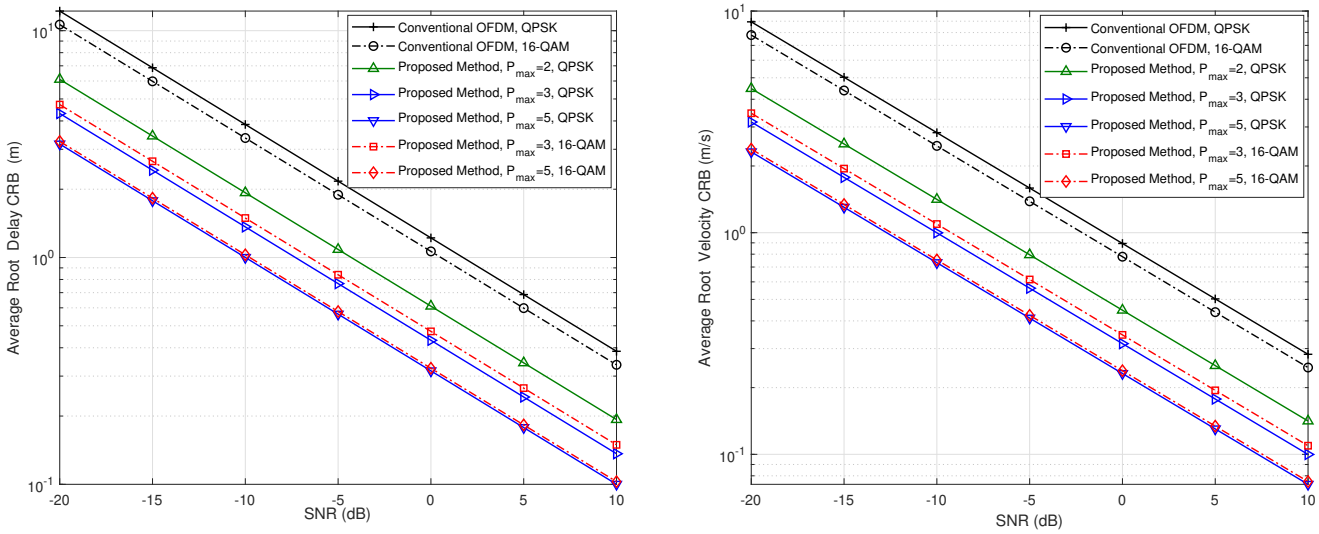



Fig. 4: The separate CRB optimization of the proposed waveform design for delay and Doppler estimation.

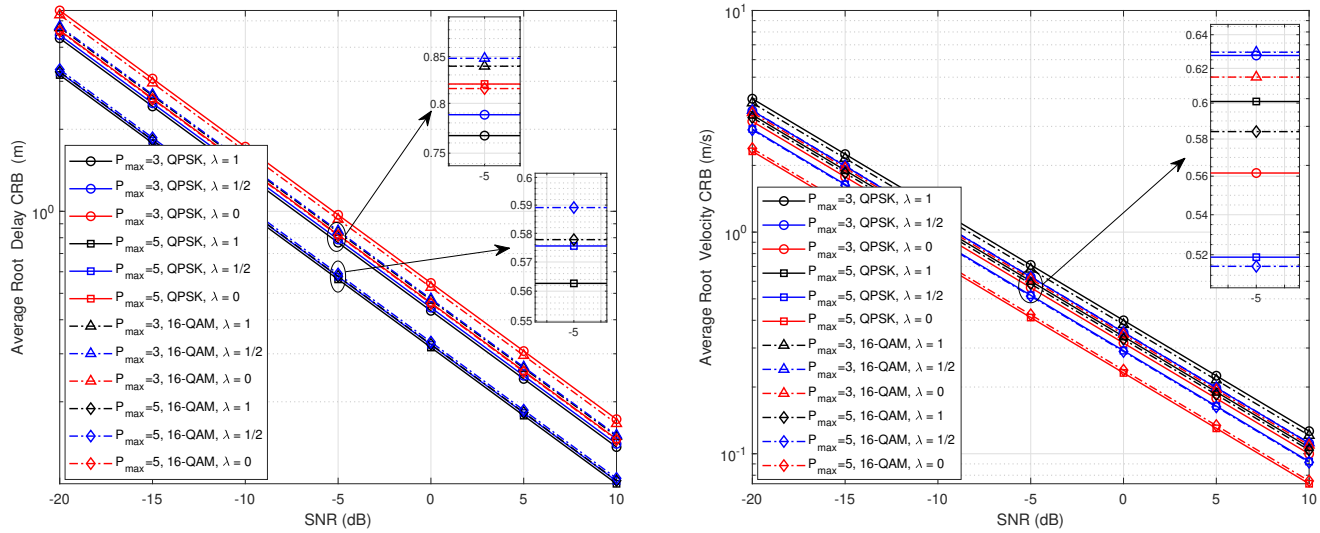



Fig. 5: The joint CRB optimization of the proposed waveform design for delay and Doppler estimation.

the average SER performance because the proposed method increases the minimum distance between the data symbols on the constellation of $D$-QAM. For the case of $P_{max} = 2$ and QPSK, there is a uniform power enhancement and the best average SER performance is obtained for this case. As result, the average SER performance in the proposed method decreases when $P_{max}$ increases as seen in Fig. 6. Although a larger $P_{max}$ decreases the average SER for data symbols on $\mathcal{C}_1$ and $\mathcal{C}_2$, their occurrence probabilities on Eqs. (32) and (33) also decrease since number of enhanced subcarriers $N_r$ decreases based on $P_max$. Moreover, when $D$ increases the average SER performance gain of the proposed method compared to conventional OFDM decreases. Lastly, the simulation results of the proposed method and conventional OFDM are verified with the analytical results in (17) and (34) as seen from the figure.

## VI. Conclusion

In this work, a novel constellation extension method is proposed to minimize the delay and Doppler CRBs for OFDM DFRC systems. The proposed method improves the radar and communication performance as being transparent to the communication receiver. The proposed waveform design involves the calculation of the total number of subcarriers for power optimization, weight matrix generation for subcarrier selection, and power allocation to decrease the CRBs. In

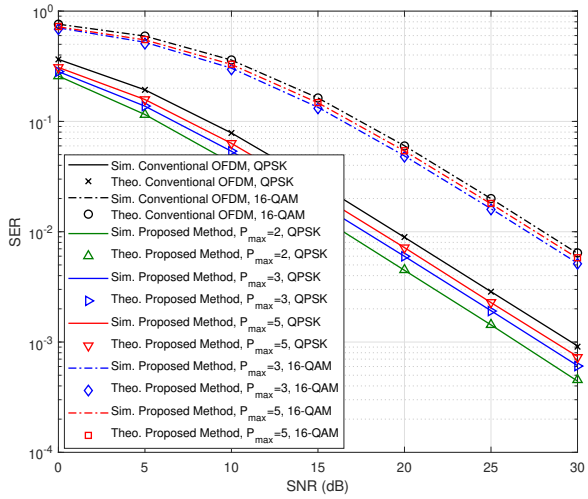



Fig. 6: SER performance of the proposed method for the comparison.

the proposed method, $\lambda$ can be adjusted according to delay and Doppler accuracy requirements. The larger $P_{max}$ values are better for the CRB minimization, but worse for average SER performance gain. Moreover, the lower $D$ values are better for the CRB minimization, but worse for average SER performance gain. For the future work, the proposed method will be modified to improve the CRBs and SER performance further under the assumption of the communication channel information at the transceiver.

## REFERENCES


[1] P. Yang, Y. Xiao, M. Xiao, and S. Li, "6G wireless communications: Vision and potential techniques," *IEEE Netw.*, vol. 33, no. 4, pp. 70–75, Jul. 2019.

[2] A. Yazar, S. Dogan-Tusha, and H. Arslan, "6G vision: An ultra-flexible perspective," *ITU J. Future Evol. Technol.*, vol. 1, no. 1, pp. 121–140, Jan. 2020.

[3] W. Saad, M. Bennis, and M. Chen, "A vision of 6G wireless systems: Applications, trends, technologies, and open research problems," *IEEE Netw.*, vol. 34, no. 3, pp. 134–142, May 2019.

[4] Y. Niu, Y. Li, D. Jin, L. Su, and A. V. Vasilakos, "A survey of millimeter wave communications (mmWave) for 5G: Opportunities and challenges," *Wireless Netw.*, vol. 21, no. 8, pp. 2657–2676, 2015.

[5] F. Liu, C. Masouros, A. P. Petropulu, H. Griffiths, and L. Hanzo, "Joint radar and communication design: Applications, state-of-the-art, and the road ahead," *IEEE Trans. Commun.*, vol. 68, no. 6, pp. 3834–3862, Jun. 2020.

[6] K. V. Mishra, M. B. Shankar, V. Koivunen, B. Ottersten, and S. A. Vorobyov, "Toward millimeter-wave joint radar communications: A signal processing perspective," *IEEE Signal Process. Mag.*, vol. 36, no. 5, pp. 100–114, Sep. 2019.

[7] L. Zheng, M. Lops, Y. C. Eldar, and X. Wang, "Radar and communication coexistence: An overview: A review of recent methods," *IEEE Signal Process. Mag.*, vol. 36, no. 5, pp. 85–99, Sep. 2019.

[8] A. R. Chiriyath, B. Paul, and D. W. Bliss, "Radar-communications convergence: Coexistence, cooperation, and co-design," *IEEE Trans. Cogn. Commun. Netw*, vol. 3, no. 1, pp. 1–12, Mar. 2017.

[9] M. L. Rahman, J. A. Zhang, X. Huang, Y. J. Guo, and R. W. Heath, "Framework for a perceptive mobile network using joint communication and radar sensing," *IEEE Trans. Aerosp. Electron. Syst.*, vol. 56, no. 3, pp. 1926–1941, Jun. 2019.

[10] P. Kumari, J. Choi, N. González-Prelcic, and R. W. Heath, "IEEE 802.11 ad-based radar: An approach to joint vehicular communication-radar system," *IEEE Trans. Veh. Technol.*, vol. 67, no. 4, pp. 3012–3027, Apr. 2017.

[11] H. Wymeersch, G. Seco-Granados, G. Destino, D. Dardari, and F. Tufvesson, "5G mmWave positioning for vehicular networks," *IEEE Wireless Commun.*, vol. 24, no. 6, pp. 80–86, Dec. 2017.

[12] C. B. Barneto, T. Riihonen, M. Turunen, M. Koivisto, J. Talvitie, and M. Valkama, "Radio-based sensing and indoor mapping with millimeter-wave 5G NR signals," in *Proc. Int. Conf. Localization GNSS (ICL-GNSS)*, Jun. 2020, pp. 1–5.

[13] C. B. Barneto, E. Rastorgueva-Foi, M. F. Keskin, T. Riihonen, M. Turunen, J. Talvitie, H. Wymeersch, and M. Valkama, "Millimeter-wave mobile sensing and environment mapping: Models, algorithms and validation," *IEEE Trans. Veh. Technol.*, vol. 71, no. 4, pp. 3900–3916, Apr. 2022.

[14] E. Memisoglu, M. M. Sahin, and H. Arslan, "Orthogonal coexistence of overlapped radar and communication waveforms," in *Proc. IEEE Wireless Commun. Netw. Conf. (WCNC)*, Apr. 2022, pp. 2190–2195.

[15] M. M. Şahin and H. Arslan, "Application-based coexistence of different waveforms on non-orthogonal multiple access," *IEEE Open J. Commun. Soc*, vol. 2, pp. 67–79, 2020.

[16] J. Qian, M. Lops, L. Zheng, X. Wang, and Z. He, "Joint system design for coexistence of MIMO radar and MIMO communication," *IEEE Trans. Signal Process.*, vol. 66, no. 13, pp. 3504–3519, 2018.

[17] T. M. Schmidl and D. C. Cox, "Robust frequency and timing synchronization for OFDM," *IEEE Trans. Commun.*, vol. 45, no. 12, pp. 1613–1621, 1997.

[18] H. Minn, V. K. Bhargava, and K. B. Letaief, "A robust timing and frequency synchronization for OFDM systems," *IEEE Trans. Wireless Commun.*, vol. 2, no. 4, pp. 822–839, 2003.

[19] A. Turlapaty, Y. Jin, and Y. Xu, "Range and velocity estimation of radar targets by weighted OFDM modulation," in *Proc. IEEE Radar Conf.*, May 2014, pp. 1358–1362.

[20] D.-W. Lim, S.-J. Heo, and J.-S. No, "An overview of peak-to-average power ratio reduction schemes for OFDM signals," *J. Commun. Netw.*, vol. 11, no. 3, pp. 229–239, Jun. 2009.

[21] T. Huang and T. Zhao, "Low PMEPR OFDM radar waveform design using the iterative least squares algorithm," *IEEE Signal Process. Lett.*, vol. 22, no. 11, pp. 1975–1979, 2015.

[22] M. Bică and V. Koivunen, "Generalized multicarrier radar: Models and performance," *IEEE Trans. Signal Process.*, vol. 64, no. 17, pp. 4389–4402, 2016.

[23] C. Sturm, T. Zwick, and W. Wiesbeck, "An OFDM system concept for joint radar and communications operations," in *Proc. IEEE Veh. Technol. Conf.*, Apr. 2009, pp. 1–5.

[24] C. Sturm and W. Wiesbeck, "Waveform design and signal processing aspects for fusion of wireless communications and radar sensing," *Proc. IEEE*, vol. 99, no. 7, pp. 1236–1259, 2011.

[25] T. Guo and R. Qiu, "OFDM waveform design compromising spectral nulling, side-lobe suppression and range resolution," in *Proc. IEEE Radar Conf.*, May 2014, pp. 1424–1429.

[26] Y. Liu, G. Liao, J. Xu, Z. Yang, and Y. Zhang, "Adaptive OFDM integrated radar and communications waveform design based on information theory," *IEEE Commun. Lett*, vol. 21, no. 10, pp. 2174–2177, 2017.

[27] Z. Zhang, Z. Du, and W. Yu, "Mutual-information-based OFDM waveform design for integrated radar-communication system in Gaussian mixture clutter," *IEEE Sens. Lett.*, vol. 4, no. 1, pp. 1–4, 2019.

[28] Y. Liu, G. Liao, Z. Yang, and J. Xu, "Multiobjective optimal waveform design for OFDM integrated radar and communication systems," *Signal Process.*, vol. 141, pp. 331–342, Dec. 2017.

[29] T. Tian, G. Li, and T. Zhou, "Power distribution for an OFDM-based dual-function radar-communication sensor," *IEEE Sens. Lett.*, vol. 4, no. 11, pp. 1–4, 2020.

[30] M. Bica, K.-W. Huang, U. Mitra, and V. Koivunen, "Opportunistic radar waveform design in joint radar and cellular communication systems," in *Proc. IEEE Global Commun. Conf.*, Dec. 2015, pp. 1–7.

[31] M. Bică and V. Koivunen, "Multicarrier radar-communications waveform design for RF convergence and coexistence," in *n Proc. IEEE Int. Conf. Acoust., Speech Signal Process.*, May 2019, pp. 7780–7784.

[32] C. Shi, F. Wang, S. Salous, and J. Zhou, "Joint subcarrier assignment and power allocation strategy for integrated radar and communications system based on power minimization," *IEEE Sensors J.*, vol. 19, no. 23, pp. 11 167–11 179, 2019.

[33] A. Ahmed, Y. D. Zhang, A. Hassanien, and B. Himed, "OFDM-based joint radar-communication system: Optimal sub-carrier allocation and power distribution by exploiting mutual information," in *Proc. Asilomar Conf. Signals Syst. Comput*, Nov. 2019, pp. 559–563.

[34] S. D. Liyanaarachchi, T. Riihonen, C. B. Barneto, and M. Valkama, "Optimized waveforms for 5G–6G communication with sensing: Theory,

simulations and experiments," *IEEE Trans. Wireless Commun.*, vol. 20, no. 12, pp. 8301–8315, 2021.

[35] M. F. Keskin, V. Koivunen, and H. Wymeersch, "Limited feedforward waveform design for OFDM dual-functional radar-communications," *IEEE Trans. Signal Process.*, vol. 69, pp. 2955–2970, 2021.

[36] B. S. Krongold and D. L. Jones, "PAR reduction in OFDM via active constellation extension," *IEEE Trans. Broadcast.*, vol. 49, no. 3, pp. 258–268, 2003.

[37] C. B. Barneto, T. Riihonen, M. Turunen, L. Anttila, M. Fleischer, K. Stadius, J. Ryynänen, and M. Valkama, "Full-duplex OFDM radar with LTE and 5G NR waveforms: Challenges, solutions, and measurements," *IEEE Trans. on Microw. Theory Techn.*, vol. 67, no. 10, pp. 4042–4054, Oct. 2019.

[38] M. Biedka, Y. E. Wang, Q. M. Xu, and Y. Li, "Full-duplex RF front ends: From antennas and circulators to leakage cancellation," *IEEE Microw. Mag.*, vol. 20, no. 2, pp. 44–55, Feb. 2019.

[39] L. Zheng and X. Wang, "Super-resolution delay-Doppler estimation for OFDM passive radar," *IEEE Trans. Signal Process.*, vol. 65, no. 9, pp. 2197–2210, 2017.

[40] M. Bică and V. Koivunen, "Radar waveform optimization for target parameter estimation in cooperative radar-communications systems," *IEEE Trans. . Aerosp. . Electron. Syst.*, vol. 55, no. 5, pp. 2314–2326, 2018.

[41] M. K. Simon and M.-S. Alouini, *Digital communication over fading channels*. New York: Wiley, 2001.

[42] J. R. Barry, E. A. Lee, and D. G. Messerschmitt, *Digital communication*. Springer Science & Business Media, 2012.

[43] J. G. Proakis, *Digital communications*. 4th ed. New York, NY: McGraw-Hill, 1998.